

# Catalytic Cracking of Methylcyclohexane over FCC Catalysts in a Mini-Fluidized CREC Riser Simulator

Mustafa Al-Sabawi and Hugo de Lasa

*Chemical Reactor Engineering Centre, Faculty of Engineering, University of Western Ontario, London, Ontario, Canada N6A 5B9*

## 1- INTRODUCTION

There is scarce information in the open literature concerning the catalytic cracking of cycloparaffins over USHY zeolites under actual fluid catalytic cracking (FCC) conditions. Cycloparaffin studies that are currently found in the literature were either conducted using fixed-bed tubular reactors, MAT-reactors or autoclaves; units that do not provide adequate simulation of large-scale FCC units in terms of reactant partial pressure, reaction contact time, temperature and catalyst/hydrocarbon ratios and fluidization regime. Moreover, limited work has been done with respect to the kinetic modeling of cycloparaffin catalytic cracking. The major concern with the present models is that they fail to consider the important effects of hydrocarbon diffusion and adsorption in the catalyst pore network, but instead, describe the combined effect of diffusion, adsorption and reaction using “pseudo-parameters”. Thus, such models are unable to define the critical role of diffusion and adsorption in FCC.

The objective of the present work is to determine the processability of methylcyclohexane (MCH) using USY catalysts with different crystallite sizes and to establish a kinetic model that accurately represents the catalytic conversion of MCH while carefully accounting for adsorption, diffusion and intrinsic kinetics. To meet such objectives, catalytic cracking experiments using MCH on USY zeolite catalysts were carried out in the mini-fluidized CREC riser simulator, a novel unit that overcomes the technical problems of the standard micro-activity test (MAT). To secure the value of the catalytic cracking of MCH, modeling studies were developed under relevant FCC process conditions in terms of partial pressures of gas oil, temperatures (450-550°C), contact times (3-7 seconds, both for the hydrocarbons and the catalyst), and catalyst-gas oil mass ratios (5), and using a well-fluidized catalyst.

## 2- EXPERIMENTATION

### 2.1- Materials

MCH (Alfa Aesar, 99% pure) catalytic cracking experiments were performed using two standard FCC catalysts, characterized by Tonetto et al.<sup>1</sup>. These catalysts were prepared using the same procedure and hence, have almost identical properties and characteristics, with the exception of the Y-zeolite crystallite size (CAT-LC and CAT-SC have 0.9  $\mu\text{m}$  and 0.4  $\mu\text{m}$  crystallites respectively). Given that the only major difference between the two catalysts is the crystallite size, quantitative evaluation of diffusional constraints could be carried out.

### 2.2- Apparatus

Thermal and catalytic cracking experiments were performed in the Chemical Reactor Engineering Centre (CREC) riser simulator using MCH. The CREC riser simulator is an experimental reactor, which operates isothermally and at constant volume of the reaction mixture, enables injected MCH reactant to vaporize and, in the case of catalytic cracking reactions, come into contact and mix with fluidized catalyst throughout a predetermined time span. Well-mixed

conditions are assumed to exist in the reactor as a result of the high gas recirculation rate. A specific description of the riser simulator components and how the system operates are presented in Al-Sabawi et al.<sup>2</sup>

Pressure transducers are installed in both the reactor and the vacuum box (VB) chambers of the unit to monitor the progress of each cracking experiment. A pressure profile in the CREC riser simulator for the catalytic cracking of MCH is shown in Figure 1. This figure shows that, prior to the injection of the feedstock into the reactor, the pressure of the reactor is 14.7 psia (1 atmosphere), whereas the VB is maintained at very low pressure (~ 1 psia). To maintain this difference in pressure, the reactor and VB are isolated by closing a four-port valve located between them. At the time of injection of MCH into the reactor, the liquid reactant rapidly vaporizes, causing an abrupt increase in pressure (A-B). Another stage follows the reactant vaporization whereby the gaseous MCH experiences cracking into different hydrocarbon products, causing an expansion in the system. As a result, a less profound pressure increase can be seen in the pressure profile (B-C). Once the preset reaction time is completed, the four-port valve is automatically switched to connect the reactor and the VB. The initial large difference in pressure between these two chambers causes the evacuation of the reaction products from the reactor into the VB. This evacuation, which occurs instantaneously due to the significant differences in pressure and volume between the reactor and VB, leads to a sudden drop in the reactor pressure, and consequent rapid pressure stabilization in both chambers (C-D). Note that any further cracking of products present in the VB is abolished due to the low temperature at which the VB is held (260°C). The pressure profiles obtained during thermal and catalytic experiments are used in determining adsorption effects, which is discussed later in this study.

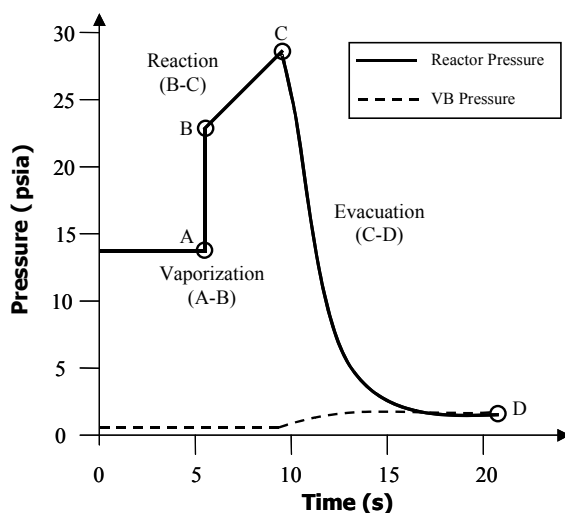


**Figure 1.** Typical pressure profile in the CREC riser simulator during a MCH catalytic cracking run. T=550°C, C/O=5

### 2.3- Experimental Conditions

Experiments involving the thermal and catalytic cracking of MCH were carried out at five temperatures of 450°C, 475°C, 500°C, 525°C and 550°C and three reaction times of 3, 5, and 7 seconds. The catalytic cracking experiments were performed using a consistent catalyst/MCH ratio of 5 (weight of catalyst = 0.81 g, weight of injected MCH = 0.162 g).

### 3- CRACKING RESULTS

#### 3.1- Thermal Cracking Results

To determine the thermal effects on the conversion of MCH, thermal cracking experiments were carried out in the CREC riser simulator at temperatures ranging from 450°C to 550°C at three reaction times of 3, 5, and 7 seconds. The MCH conversion was determined at each condition, and these conversions were found to be quite significant, especially at high temperatures (550°C) and 7 seconds contact time, under which the overall conversion exceeds 4 wt%. What makes thermal cracking even more relevant is given by the fact that catalytic cracking experiments performed under similar reaction temperatures using a USY zeolite catalyst provided overall conversions of about 16 wt%. Hence, thermal cracking should not be neglected when examining the processability and the kinetic modeling of MCH, and cycloparaffins in general, during FCC operation.

#### 3.2- Catalyst Activity Results - Overall MCH Conversion

An important objective of this study is to determine MCH conversions at typical catalytic cracking conditions using the two catalysts, CAT-LC and CAT-SC, and to ascertain the effect of diffusion on the overall cracking of MCH. It is observed that MCH conversions increased with both temperature and reaction time. Figures 2 and 3 illustrate this trend for CAT-LC and CAT-SC, respectively. For instance, for experiments conducted at 500°C seconds using CAT-LC, the MCH conversions are 8.7, 10.9 and 13.0 wt % at reaction 3, 5 and 7 seconds, respectively. In this respect, a 2-wt% rise in MCH conversion was detected when the reaction time was increased from 3 to 5 seconds as well as from 5 to 7 seconds. Similar trends are observed using CAT-SC. It is important to note that the MCH conversion values reported in Figures 2 and 3 are averages obtained using at least four repeat experiments at each of the reaction conditions proposed in this study. Typical errors for the MCH conversion reached up to about 1.3 wt%.

It is observed that increasing the temperature for a given reaction time causes a steady increase in the overall MCH conversion. On this basis, it is possible to assume that the catalytic cracking reaction under the conditions of the CREC riser simulator displayed an apparent activation energy that did not change with temperature. Furthermore, while examining MCH conversions on USY catalysts, it is apparent that the overall rate of conversion is not affected by pore diffusion resistance within the crystallite network. This would seem to be the case as the larger zeolite crystallites provided slightly higher MCH conversions than their smaller counterparts. With its smaller zeolite crystallites, CAT-SC would have provided higher MCH conversions in the case where the reaction rate is influenced by internal mass transfer limitations. These observations, along with the constant apparent activation energy over the studied temperature range, confirm that MCH is not diffusionally controlled within the crystallite pore network. This claim is further validated by our research group using model compounds having larger critical diameters than MCH in experiments performed under similar conditions and using the same catalysts.<sup>3,4</sup> Nonetheless, even if there were mass transport limitations, diffusion parameters can be assessed independently of adsorption and reaction kinetic parameters using a methodology similar to the one established by Al-Sabawi et al.<sup>2</sup>

Small variations in MCH conversions (~2-3%) between the two catalysts can be explained by the differences in their acidity. Although these differences are minor (about 10%), CAT-LC possesses a higher Brønsted-to-Lewis sites ratio than its CAT-SC counterpart.<sup>1</sup> It is well-known that the higher the zeolite acidity, the more cracking exists, since cracking reactions proceed based on a single site occupancy mechanism.<sup>5</sup>

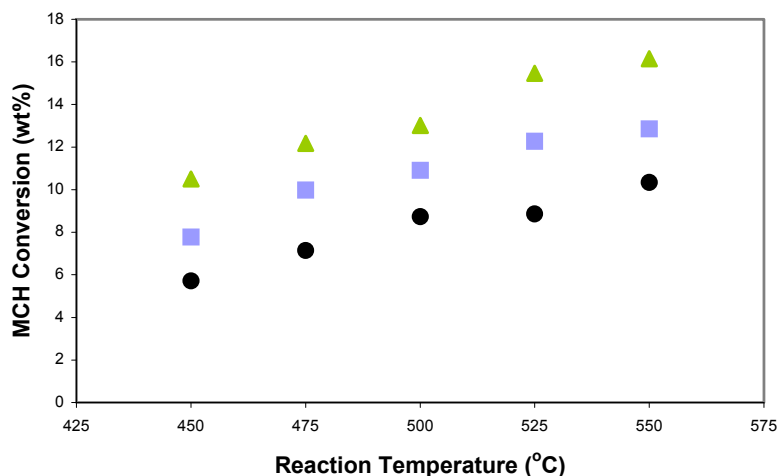


**Figure 2.** Conversion of MCH over CAT-LC at different temperatures. Experiments were conducted at reaction times of 3 seconds (●), 5 seconds (■) and 7 seconds (▲) using a catalyst-gas oil ratio of 5.

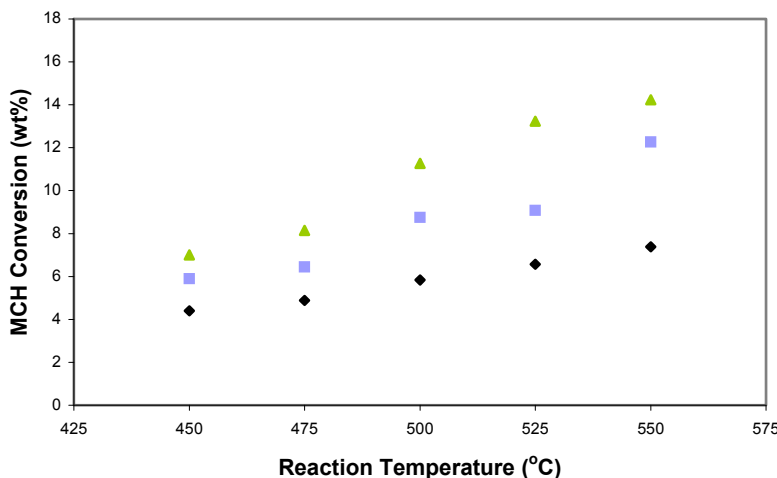


**Figure 3.** Conversion of MCH over CAT-SC at different temperatures. Experiments were conducted at reaction times of 3 seconds (●), 5 seconds (■) and 7 seconds (▲) using a catalyst-gas oil ratio of 5.

### 3.3- MCH Reaction Mechanisms

Products formed during MCH conversion were analyzed by GS-MS after each thermal and catalytic cracking experiment. Over 60 product species were detected. Based on the observable hydrocarbon products obtained, analysis of product yield plots<sup>6</sup> and reaction mechanisms and pathways reported in the literature,<sup>6,7,8</sup> a reaction scheme can be proposed for the catalytic conversion of MCH using USY zeolites in the CREC riser simulator. This reaction scheme is presented in Figure 4. It is important to note that MCH can undergo several types of reactions, including ring opening, cracking, isomerization, hydrogen transfer, transalkylation and dealkylation.

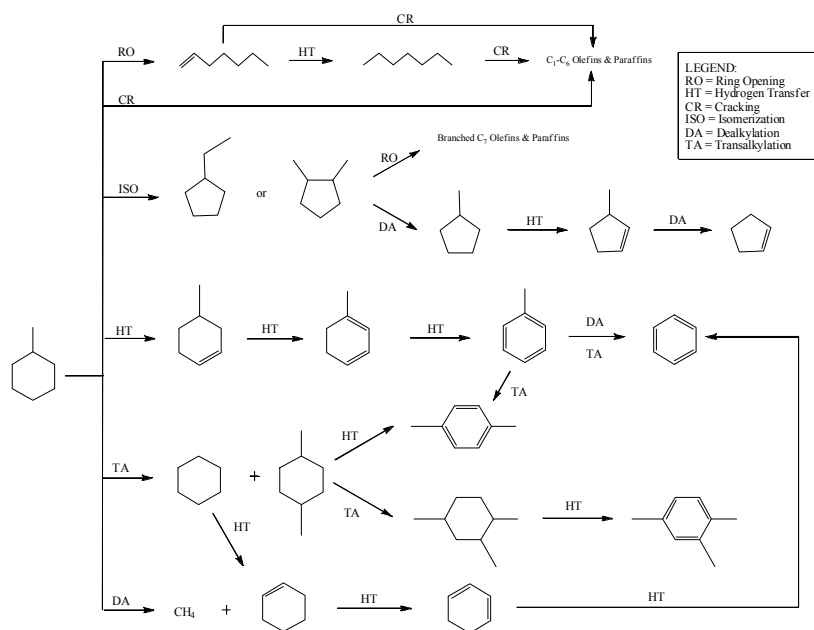


**Figure 4.** Simplified reaction scheme for the catalytic cracking of MCH based on observable products

#### 4- MODELING DIFFUSION, ADSORPTION AND REACTION PHENOMENA

Since the development of a kinetic model to describe MCH conversion is a complex process, taking a practical and effective approach becomes essential in order to establish a model that accurately describes MCH conversion. The approach taken in this study involves using observable hydrocarbon product species as well as the main MCH reaction mechanisms and pathways reported in Figure 4. Thus, a simplified kinetic model that accurately describes MCH catalytic conversion may be developed, as presented in Figure 5. This model considers primary reactions, including (i) ring opening and cracking of MCH into heptene and olefins with seven carbons or less; (ii) isomerization of MCH into 5-carbon ring compounds, including ethylcyclopentane and dimethylcyclopentane; (iii) dealkylation of MCH, forming cyclohexene and methane; and (iv) transalkylation of MCH into larger C<sub>8</sub> and C<sub>9</sub> cycloparaffins. The abundant amounts of aromatics formed, such as toluene, benzene, xylene and other C<sub>8</sub> and C<sub>9</sub> aromatic compounds makes it necessary to include four other secondary reactions in the proposed model: (v) hydrogen transfer between MCH and olefins resulting in the saturation of olefins into paraffins and the dehydrogenation of MCH into methylcyclohexene, methylcyclohexadiene and toluene; (vi) transalkylation of toluene to produce benzene and xylene; (vii) hydrogen transfer between C<sub>8</sub> and C<sub>9</sub> cycloparaffins and olefins leading to the production C<sub>8</sub> and C<sub>9</sub> aromatics and paraffins; and (viii) hydrogen transfer between cyclohexene and olefins, resulting in the formation of benzene and paraffins. The majority of the catalytic cracking products detected are included in this model. Note that the transalkylation of toluene (reaction vi) was incorporated in the kinetic model due to the observed consumption of toluene.<sup>6</sup>

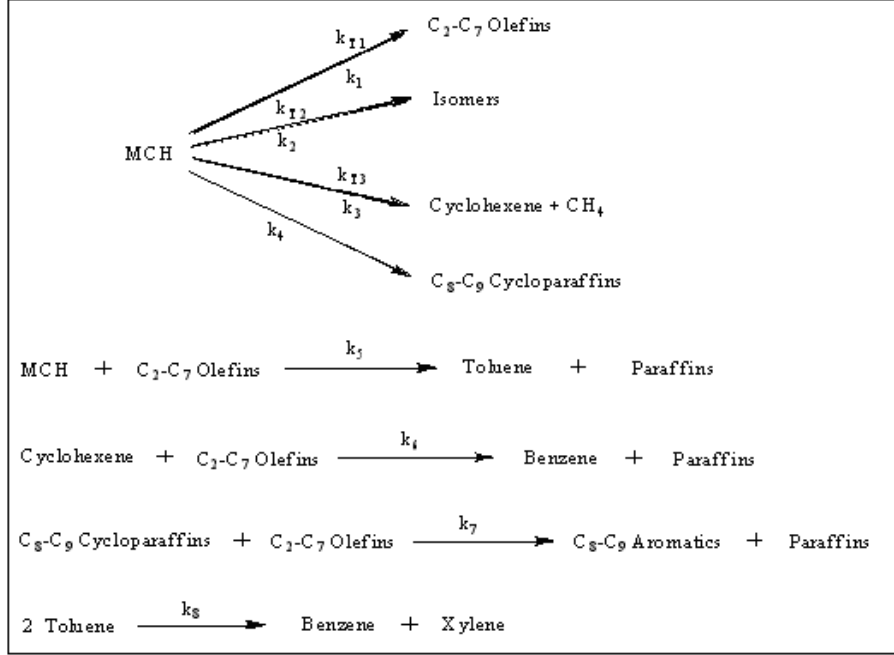


**Figure 5.** Proposed MCH catalytic conversion model

MCH conversion through reactions (i), (ii) and (iii) can be modeled by first order kinetics, since the kinetic order of cracking single molecules is unity<sup>9</sup> and since all of these types of reactions are unimolecular. Transalkylation and hydrogen transfer reactions, on the other hand, described by reactions (iv), (v), (vi), (vii) and (viii) are modeled by second-order kinetics, since two molecules are involved in these mechanisms.

It is important to also consider products formed via thermal cracking during the catalytic cracking runs, since it was already shown that thermal effects play a substantial role in the conversion of MCH. Determination of thermal cracking products indicates that the overwhelming majority of the products were formed via cracking, ring opening, isomerization and dealkylation. Since transalkylation and hydrogen transfer are bimolecular reactions that usually require the presence of a catalyst to take place, products from these reactions were very limited during thermal experiments and therefore, were not included in the overall model. The thermal kinetic parameters ( $k_{T1}$ ,  $k_{T2}$ ,  $k_{T3}$ ) are included in Figure 5 along with the catalytic parameters.

In order to take into account diffusion and adsorption phenomena, several equations must be considered and incorporated in the set of model rate equations. Firstly, a “quasi-steady state” effectiveness factor,  $\eta_{ss}$ , which accounts for diffusion of reactant species through the zeolite pore network, can be defined as:

$$\eta_{ss} = \frac{r_{mean}}{-k_i C_{i,in}^2 \Big|_{r=R_{cr}}} \quad (1)$$

where  $k_i$  is the intrinsic kinetic constant,  $r_{mean}$  is the observed rate of consumption/formation,  $C_{i,in}$  are the reactant concentration inside the crystallite,  $r$  is the crystallite radial coordinate and  $R_{cr}$  is the crystallite radius. Thus, the disappearance of MCH in the well-mixed mini-fluidized CREC riser simulator can be represented by the following species balance equation:

$$\frac{V}{W_{cr}} \frac{dC_A}{dt} = \eta_{ss} r_A \quad (2)$$

where  $r_A$  is the rate of the consumption of MCH in the absence of diffusion control,  $C_A$  represents the concentration of MCH in the gas phase,  $V$  is the volume of the riser simulator and  $W_{cr}$  is the mass of crystallites. The complete derivation of this equation is presented by Al-Sabawi et al.<sup>6</sup>

Moreover, one can also argue on the basis of adsorption thermodynamics that each adsorption constant for species  $i$  is exponentially related to the corresponding reaction temperature as:

$$K_i = K_{i0} \exp\left(\frac{-\Delta H_i}{RT}\right) \quad (3)$$

where  $K_{i0}$  is the pre-exponential factor with units of  $\text{m}^3/(\text{kg of catalyst})$  and  $\Delta H_i$  is the heat of adsorption in  $\text{kJ/mol}$ . Performing thermal and catalytic experiments in a range of temperatures and using equation (3) allows the independent assessment of adsorption parameters, as will be discussed later.

Considering a Langmuir-Hinselwood representation of the adsorption of species on the catalyst active sites and that the ideal gas law applies, the design equation for the thermal and catalytic cracking of MCH in the CREC riser simulator can be expressed by the following equation:

$$-V \frac{dC_A}{dt} = \eta_{ss} \varphi_{\text{int}} W_{cr} \left[ \frac{K_A}{1 + K_A C_A} (k_1 + k_2 + k_3) C_A + \frac{2K_A}{(1 + K_A C_A)^2} k_4 C_A^2 + \frac{K_A K_B}{(1 + K_A C_A + K_B C_B)^2} k_5 C_A C_B \right] + V k_{T1,2,3} C_A \quad (4)$$

where  $k_1, k_2, k_3, k_4$  and  $k_5$  are the intrinsic kinetic constant, associated with the reactions shown in Figure 5,  $k_{T1,2,3}$  is the overall thermal intrinsic kinetic constant associated with the MCH thermal cracking which combines all thermal constants presented in Figure 5,  $K_A$  and  $K_B$  represent the adsorption constants for MCH and olefins respectively, and  $\varphi_{\text{int}}$  is the catalyst activity decay function.

Furthermore, each thermal and catalytic intrinsic kinetic constant,  $k_i$ , can be postulated to change with the reactor temperature,  $T$ , following a re-parameterized Arrhenius-type equation:

$$k_i = k_{i0} \exp\left(\frac{-E_i}{R} \left(\frac{1}{T} - \frac{1}{T_0}\right)\right) \quad (5)$$

where  $E_i$  represents the energy of activation,  $k_{i0}$  is the pre-exponential factor, and  $T_0$  is the centering temperature defined as the average temperature used in the reaction experiments, which is  $500^\circ\text{C}$ .

It is well-known that the deposition of coke on the catalyst surface decreases the catalyst activity, since coke covers the active sites of the catalyst. Catalyst activity decay function,  $\varphi_{\text{int}}$ , can be accounted for relating catalyst activity to the coke concentration on the catalyst, as suggested by Froment and Bischoff.<sup>10</sup> Thus,  $\varphi_{\text{int}}$  can be evaluated by the following expression:

$$\varphi_{\text{int}} = \exp(-\lambda X'_{\text{coke}}) \quad (6)$$

where  $\lambda$  is the deactivation parameter for MCH cracking and  $X'_{\text{coke}}$  represents the mass of coke produced per mass of MCH injected. The present kinetic model does not consider the effect of coke on adsorption processes. Adsorption parameters are not assumed to depend on the amount of coke produced. This assumption is based on results published by Atias et al.<sup>11</sup> who found that

adsorption constants and available surface area remain somewhat constant at low levels of coke. Coke analysis will be discussed in the modeling section of this paper.

In addition to the equations already presented, rate equations can be derived for each product fraction in Figure 5 (olefins, isomers, cyclohexene, C<sub>8</sub>-C<sub>9</sub> cycloparaffins, toluene, benzene, C<sub>8</sub>-C<sub>9</sub> aromatics and xylene), taking into account their formation and/or consumption.

## 5- ASSESSMENT OF ADSORPTION PARAMETERS IN THE CREC RISER SIMULATOR

A set of thermal and catalytic experiments at various temperatures were performed to assess the adsorption parameters of decalin on typical FCC Y-zeolite catalysts. The adsorption constants of MCH were experimentally calculated from the pressure profile recorded in experiments carried out with and without catalyst loaded in the CREC riser simulator. Comparing the pressure attained at the end of the vaporization period for a thermal and a catalytic experiment (point 'B' in Figure 1), the difference between pressures represents the fraction of reactant adsorbed on the catalyst. This approach is valid assuming that adsorption equilibrium is achieved almost instantaneously. The equation for the determination of the adsorption constant of species *i*,  $K_i$ , can be expressed by the following (see Al-Sabawi et al.<sup>6</sup> for derivation):

$$K_i = \frac{(P_i^{thermal} - P_i^{catalytic}) V}{(P_i^{catalytic} - P_{atm}) m_{cat}} \quad (7)$$

where  $P_i^{thermal}$  and  $P_i^{catalytic}$  are the total pressure at the moment of vaporization (point 'B' in Figure 1) for the thermal and the catalytic experiments respectively,  $P_{atm}$  is the initial pressure (=14.7 psia),  $m_{cat}$  is the mass of catalyst used during catalytic experiments and  $V$  is the volume of the CREC riser simulator reactor.

Equation (7) allows for the calculation of adsorption constants at initial conditions of the catalytic reaction as a decoupled calculation of the kinetic parameters. Therefore, assessment of adsorption constants through equation (7) requires pressure profiles of both the thermal and the catalytic runs under the same conditions. The assumptions behind the derivation of equation (7) are presented in Al-Sabawi et al.<sup>6</sup>.

Adsorption constants for MCH were evaluated at different temperatures, ranging from 350°C to 550°C for CAT-LC. Performing experiments in a range of temperatures provides the use of equation (3) to assess the heat of adsorption using linear regression technique. A centering temperature  $T_0$  (723 K) was used to assess parameters with low cross-correlation. Figure 6 reports adsorption constants for MCH at various temperatures. Given the exothermic nature of adsorption, the adsorption constants are expected to decrease with temperature. The pre-exponential adsorption constant and heats of adsorption were found to be  $[10.35 \pm 0.58] \times 10^{-6}$  [m<sup>3</sup>/(kg of catalyst)] and  $-40.36 \pm 2.26$  (kJ/mol) respectively.



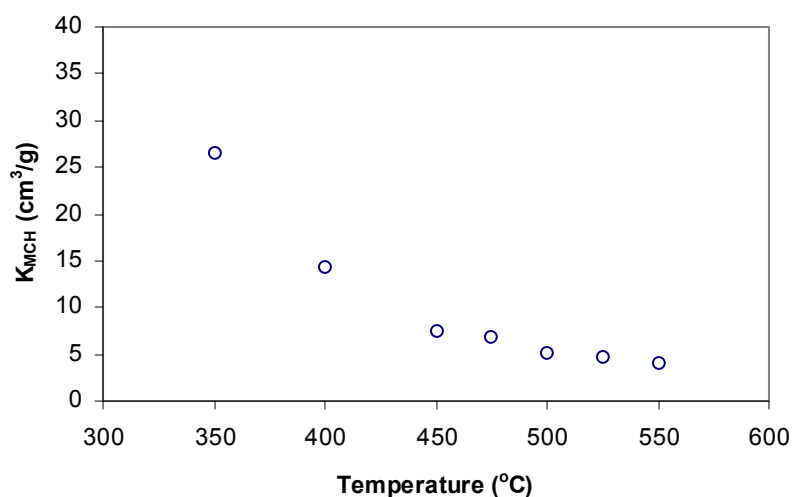


**Figure 6.** Adsorption constants for MCH at different temperatures over CAT-LC

It is important to note that the adsorption constants for each of the product species participating in the reactions shown in Figure 5 were also determined using the same methodology of evaluating the decalin adsorption parameters.

## 6- EVALUATION OF INTRINSIC KINETIC PARAMETERS

Given that the adsorption parameters were already calculated in previous section of this study, the intrinsic thermal kinetic parameters ( $k_{T1}$ ,  $k_{T2}$ ,  $k_{T3}$ ,  $E_{T1}$ ,  $E_{T2}$ ,  $E_{T3}$ ) and intrinsic catalytic kinetic parameters ( $k_{10} - k_{80}$ ,  $E_1 - E_8$ , and  $\lambda$ ) can be assessed to fully characterize the adsorptive-reactive system. This sequential methodology of parameter estimation leads to adsorption parameters with smaller spans than the intrinsic kinetic parameters because of the propagation of errors.

As previously mentioned, the overall rate of MCH conversion is controlled via intrinsic kinetic and is not hindered by MCH diffusion within the USY crystallites. Therefore, the effectiveness factor term that was included in the proposed modeling equations to factor in the diffusion phenomenon can be set equal to one.

Moreover, measurement of the amount of coke deposited on the catalyst active sites under worst-case reaction conditions (i.e. at highest reaction temperature (550°C) and longest reaction time (7 seconds)) revealed coke levels equal to 0.29 wt%. Since coke yields obtained under all other experimental conditions are less than this amount, the deactivation parameter,  $\lambda$ , can be considered to be negligible for modeling purposes.

Following these simplifications, the proposed kinetic model includes 22 intrinsic kinetic parameters (6 for thermal conversion and 16 for catalytic conversion) that are to be assessed. Applying non-linear regression techniques to data (yields of each product and unconverted MCH) obtained from thermal runs in the riser simulator, along with thermal rate equations for each of the species in Figure 5 allows for the independent evaluation of the six thermal cracking kinetic constants from other model parameters. These thermal constants are reported in Table (1).

The thermal constants were then incorporated into the evaluation of the remaining 16 catalytic parameters. Nonlinear regression was performed to determine these constants using experimental data of MCH catalytic conversions at temperatures ranging from 450°C to 550°C

and at reaction times of 3, 5 and 7 seconds. The function of residuals is minimized using the large-scale algorithm based on the interior-reflective Newton method described in Coleman and Li.<sup>12</sup>

Table 1 also reports the catalytic intrinsic kinetic parameters obtained using CAT-LC, along with the corresponding 95% confidence limits. Little cross-correlation between the fitted parameters was observed,<sup>6</sup> and this statistically describes the low level of interaction between the calculated parameters.

It is also important to note that most of the 95% confidence limits calculated for each parameter are moderate (below 39%), indicating that the fittings obtained are accurate. However, the 95% confidence interval of the activation energy associated with the transalkylation of toluene (i.e.  $E_8$ ) was greater than the calculated value of this parameter, indicating that the kinetic constant,  $k_8$ , is statistically insignificant and may be eliminated from the model. This observation shows that the disproportionation of toluene into benzene and xylene is a trivial reaction and that toluene is involved in other reactions that allow for its consumption. Toluene may in fact experience dealkylation, instead of transalkylation, to form benzene.

A comparison of the intrinsic activation energies values for primary MCH reactions determined that the catalytic cracking and ring opening of a MCH molecule involves a higher energy of activation than isomerization (74 versus 50 kJ/mol). Thus, an increase in temperature leads to a larger fraction of heptene and smaller cracking products. The lower activation energies reported for the isomerization of MCH indicate that isomerization reactions are less sensitive to temperature variations. Thus, isomer formation does not change significantly with temperature.

The intrinsic activation energies obtained for the catalytic conversion reaction of MCH ( $E_1 - E_4$ ) was in the 50-79 kJ/mol range. Addition of these intrinsic activation energy values to the heat of adsorption assessed earlier for MCH (-40 kJ/mol) yields overall energies of activation ranging from 10-39 kJ/mol.

**Table 1.** Intrinsic Kinetic Parameters for MCH Thermal and Catalytic Conversion

Thermal Parameters			Catalytic Parameters		
	Value	95% CFL		Value	95% CFL
$k_{T10}$ (1/s)	0.0889	0.0058	$k_{10}$ (1/s)	6.741	0.077
$E_{T1}$ (kJ/mol)	68.80	12.00	$E_1$ (kJ/mol)	73.78	1.44
$k_{T20}$ (1/s)	0.0148	0.0038	$k_{20}$ (1/s)	2.218	0.055
$E_{T2}$ (kJ/mol)	50.28	44.44	$E_2$ (kJ/mol)	49.55	2.24
$k_{T30}$ (1/s)	0.0215	0.0043	$k_{30}$ (1/s)	0.386	0.084
$E_{T3}$ (kJ/mol)	42.75	33.71	$E_3$ (kJ/mol)	53.61	19.69
			$k_{40}$ (m <sup>3</sup> /mol/s)	0.016	0.001
			$E_4$ (kJ/mol)	73.50	8.46
			$k_{50}$ (1/mol/s)	1.779x10 <sup>8</sup>	9.498x10 <sup>6</sup>
			$E_5$ (kJ/mol)	81.33	6.94
			$k_{60}$ (1/mol/s)	2.507x10 <sup>12</sup>	1.311x10 <sup>12</sup>
			$E_6$ (kJ/mol)	113.01	37.01
			$k_{70}$ (1/mol/s)	3.103x10 <sup>10</sup>	4.442x10 <sup>9</sup>
			$E_7$ (kJ/mol)	87.64	21.18
			$k_{80}$ (1/mol/s)	1.378x10 <sup>8</sup>	4.251x10 <sup>7</sup>
			$E_8$ (kJ/mol)	10.83	44.07

## 7- CONCLUSION

The contributions of the present study can be summarized as follows:

- (a) Reaction pathways of MCH and its products were determined, confirming those proposed by previous studies conducted outside FCC conditions.
- (b) A heterogeneous kinetic model for the catalytic cracking of MCH describing thermal effects as well as adsorption and reaction phenomena, applicable in the context of the CREC riser simulator, was established. Using non-linear regression and statistical parameter estimation techniques, kinetic parameters were determined, including thermal and primary catalytic intrinsic activation energies, which were in the range of 42-69 kJ/mol and 49-74 kJ/mol, respectively.
- (c) Adsorption constants for MCH on USY zeolite catalyst were assessed under typical catalytic cracking reaction conditions. The exothermic nature of MCH adsorption was confirmed, with the heat of adsorption being – 40 kJ/mol.
- (d) MCH is not diffusionally limited under relevant FCC conditions. MCH's small critical molecular size allows for easy MCH transport through the zeolite catalyst pore network.

---

<sup>1</sup> Tonetto, G.; Atias, J. A.; de Lasa, H. FCC Catalysts with Different Zeolite Crystallite Sizes: Acidity, Structural Properties and Reactivity. *Appl. Catal., A*. **2004**, *270*, 9-25.

<sup>2</sup> Al-Sabawi, M.; Atias, J.A.; de Lasa, H. Kinetic Modeling of Catalytic Cracking of Gas Oil Feedstocks: Reaction and Diffusion Phenomena. *Ind. Eng. Chem. Res.*, **2006**, *45*, 1583-1593.

<sup>3</sup> Atias, J.A.; Tonetto, G.; de Lasa, H.I. Catalytic Conversion of 1,2,4-Trimethylbenzene in a CREC Riser Simulator. A Heterogeneous model with Adsorption and Reaction Phenomena. *Ind. Eng. Chem. Res.* **2003**, *42*, 4162-4173.

<sup>4</sup> Atias, J.A.; de Lasa, H. Adsorption and Catalytic Reaction in FCC Catalysts using a Novel Fluidized CREC Riser Simulator. *Chem. Eng. Sci.* **2004**, *59*, 5663-5669.

<sup>5</sup> de la Puente, G. and Sedran, U., Conversion of Methylcyclopentane on Rare Earth Exchanged Y Zeolite FCC Catalysts, *Applied Catalysis*, **1996**, *144*, 147.

<sup>6</sup> Al-Sabawi, M.; de Lasa, H. Kinetic Modeling of Catalytic Conversion of Methylcyclohexane over USY zeolites: Adsorption and Reaction Phenomena. Manuscript in preparation.

<sup>7</sup> Corma, A.; Gonzalez-Alfaro, V.; Orchilles, A.V. Decalin and Tetralin as Probe Molecules for Cracking and Hydrotreating the Light Cycle Oil. *Journal of Catalysis*, **2001**, *200*, 34-44.

<sup>8</sup> Cerqueira, H.S.; Mihindou-Koumba, P.C.; Magnoux, P.; Guisnet, M. Methylcyclohexane Transformation Over HFAU, HBEA and HMF1 Zeolites: I. Reaction Scheme and Mechanisms. *Ind. Eng. Chem. Res.*, **2001**, *40*, 1032.

<sup>9</sup> Van Landeghem, F.; Nevicato, D.; Pitault, I.; Forissier, M.; Turlier, P.; Derouin, C.; Bernard, J.R. Fluid Catalytic Cracking: Modelling of an Industrial Riser. *Appl. Catal. A: Gen.* **1996**, *138*, 381-405.

<sup>10</sup> Froment, G.F.; Bischoff, K.B. *Chemical Reactor Analysis and Design (2nd Ed.)*; New York: Wiley, 1979.

<sup>11</sup> Atias, J. A.; Tonetto, G.; de Lasa, H. Modeling Fluid Catalytic Cracking in a Novel CREC Riser Simulator: Adsorption Parameters under Reaction Conditions. *Int. J. Chem. React. Eng.* **2003**, *1* (A-50), 1-25.

<sup>12</sup> Coleman, T. F.; Li, Y. An Interior, Trust Region Approach for Nonlinear Minimization Subject to Bounds. *SIAM J. Optim.* **1996**, *6*, 418-445.